

# Structure Identification and Detection for the Unsteady Separated Flow

Anotai Suksangpanomrung

Department of Mechanical Engineering, Chulachomklao Royal Military Academy  
Maung, Nakhorn-Nayok, 26001

Tel: (037) 393010-4 ext 62305, Fax: (037)393487, E-mail: asuksang@hotmail.com

## Abstract

In computational fluid dynamics, the post-processing process is considered to be an important step since it help us to analyze and visualize the details of the flow that we have studied. For the separated flow, coherent structures which exist in the flow, play a significant role. It has become increasingly evident that coherent structure influence mixing, noise, vibration, heat transfer, drag etc. In this paper, we overview the state of the art of detecting and identifying the flow structure such as a one-dimensional wavelet transform and Fourier spectral analysis, a lambda II ( $\lambda_2$ ) and typical  $|\omega|$  approaches. These techniques are applied to the unsteady flow over a bluff rectangular plate.

The wavelet analysis offers an alternative approach to the problem of detecting and identifying the flow structure. It provides not only the spectral information, as in Fourier spectral analysis, but also localization of events in time. For structure identification, the flow structure is clearly identified with the  $\lambda_2$  technique than the typical  $|\omega|$  technique and identical to the experimental sketch.

## 1. Introduction

From a computational view point, the most problematic aspect of turbulence is the wide range of turbulent eddy sizes. The size and structure of the largest eddies depend on the flow condition and configuration (geometry). While the small eddies are much more universal and have less impact on the flow. Turbulence can be viewed as a tangle of vortex filament and much of turbulence physics is explained using the concept of vortex dynamics. Many turbulent shear flows, such as mixing layer, turbulent jet, wakes and boundary layer, have been found to be dominated by spatially coherent, temporally evolving, vortical motions, usually called **coherent structure**. These structures can be identified by the concentration of large-scale vorticity and significant energy level and organized by a mean velocity gradient [1]. Such structures are very important for understanding turbulence phenomena since they responsible for a large part of entrainment and mixing, heat and mass transfer, chemical reaction, drag, aerodynamic noise generation and modeling of turbulence.

A distinction can be make between near-wall and core structures. An example of core structures are the large eddies usually associated with shear layer instability such as Kelvin-Helmholtz type instability [2], or shedding type instability. In near-wall region, the concept

of coherent structures had lead to a detailed description and mechanism of the phenomena responsible for the production and the transport of turbulence. Typical coherent structures in near-wall region include hairpin (horseshoe) vortices, bursts and streaks.

For detecting the information of this coherent structure, it is possible to classify into two approaches, the conditional and the statistical approach [1]. The first approach consists of detecting from some condition the passage or presence of a given event. This detection allows us to collect events, to compute averages and then to build the main characteristics of the coherent structure. The second approach involved statistical information in order to derive the characteristics of the coherent structure such as the space-time correlation. For identifying the coherent structure, if we limit the identification to only the vortex core, four methods had been summarized by J. Jeong and F. Hussain [3]

The objective of this paper is to overview the state of the art of detecting and identifying techniques and apply some techniques such as the one-dimensional wavelet transform analysis, a lambda II ( $\lambda_2$ ) analysis to the unsteady flow over a bluff rectangular plate. These numerical simulations have been successfully simulated in the past in two and three-dimensional computational domains with DNS and LES techniques in a wide range of Reynolds numbers [4]

## 2. Structure Identification/Detection

### 2.1 Structure detecting techniques

Two techniques will be investigated in this paper, the classical Fourier spectral approach and the one-dimensional wavelet transform approach. Wavelet analysis has been used in recent years with considerable success in variety of fields. The main advantage is the decomposition of an arbitrary signal into contributions that are localized in both time and scale (frequency). In the classical Fourier analysis, on the other hand, local fluctuation occurring only over a short duration or intermittently contributes to the spectrum computed over the entire period of integration and for short duration or intermittent events, information on their occurrence on the time axis is lost. Wavelet analysis retains this information and can be particularly useful in investigating phenomena that are non-stationary, have a short-lived transient component and that are characterized by

different scales. The application of wavelet transform analysis to turbulent flows has been reviewed by Farge [5]. The technique was recently used to analyze the vortical structure in the wake of a bluff body [6] and in a plane mixing layer [7].

We will briefly outline the background on the one-dimensional continuous wavelet transform used in this investigation. Details on other wavelet transforms and applications are available in [5] and in a number of review papers on the World Wide Web. The continuous wavelet transform is a linear integral transform that associates a function  $Wf(s, \tau)$  with a signal  $g(t)$  and  $\psi_{s, \tau}$  according to the definition;

$$Wf(s, \tau) = \int_{-\infty}^{\infty} \psi_{s, \tau}^*(t) g(t) dt \quad (1)$$

and

$$\psi_{s, \tau}^*(t) = \left( \frac{1}{\sqrt{s}} \right) \psi \left( \frac{t - \tau}{s} \right) \quad (2)$$

Where  $Wf(s, \tau)$  is the wavelet transform function and  $g(t)$  is a time series signal.  $\psi(t)$  is the basic analyzing wavelet (also refereed to as “mother wavelet”). Stretching (or dilating) by the scale  $s$  and translating with location  $\tau$ , this mother wavelet yields a “daughter wavelet”,  $\psi_{s, \tau}(t)$ . The asterisk (\*) denotes its complex conjugate. The normalizing constant  $(\frac{1}{\sqrt{s}})$  is chosen so that the energy in the dilated wavelet function is the same for all scale. The wavelet energy spectrum can be defined as a distribution of the energy in the signal  $g(t)$  over the wavelet scales. This form allows the energy in each wavelet scale to be interpreted in a manner analogous to the Fourier energy spectrum.

$$E(s) = \int_{-\infty}^{\infty} |Wf(s, \tau)|^2 d\tau \quad (3)$$

Since the wavelet transform is an energy preserving transformation, we can define the total energy in the signal as

$$E_t = \int_{-\infty}^{\infty} |g(t)|^2 dt = \frac{1}{s^2 C_\psi} \int_0^\infty E(s) ds \quad (4)$$

where the constant  $C_\psi$  depends on the mother wavelet. In this study, two wavelet families are selected for the mother wavelet, the Morlet and the Mexican hat wavelet. The Morlet wavelet provides good spectral accuracy and is useful for detecting periodicity in the signal. Information about both amplitude and phase can be extracted since the wavelet is complex. The Morlet wavelet is given by;

$$\psi(t) = e^{-t^2/2} \left( e^{-i\omega_0 t} - e^{-\omega_0^2/2} \right) \quad (5)$$

For  $\omega_0 \geq 5$ , the last term in (5) is negligible. Therefore the Morlet wavelet can be approximated as;

$$\psi(t) = e^{-t^2/2} e^{-i\omega_0 t} \quad (6)$$

The Mexican hat is the classical second derivative of the Gaussian function and is defined as,

$$\psi(t) = (t^2 - 1)e^{-t^2/2} \quad (7)$$

The Mexican hat wavelet is good for detecting local increase or decrease of the signal and the localization of inflexion points (edges or the discontinuity point).

## 2.2 Structure identifying techniques

According to Jeong and Hussain [3], four methods had been proposed, a lambda II ( $\lambda_2$ ), delta ( $\Delta$ ), Q and  $|\omega|$  techniques. In present study, we will identify and compare the flow structure between the lambda II ( $\lambda_2$ ) and  $|\omega|$  techniques. For lambda  $\lambda_2$  technique, the vortex cores are extracted directly from the instantaneous velocity fields and identified with a region of negative  $\lambda_2$ , the second largest eigenvalue of the tensor  $S_{ik}S_{kj} + \Omega_{ik}\Omega_{kj}$ , where  $S_{ij} = (U_{i,j} + U_{j,i})/2$  and  $\Omega_{ij} = (U_{i,j} - U_{j,i})/2$  are the symmetric and antisymmetric parts of the velocity gradient tensor,  $u_{i,j} = \frac{\partial u_i}{\partial x_j}$ . This method has been successful in capturing vortical structures, even in the presence of strong shear occurring in near wall boundary layers [8]

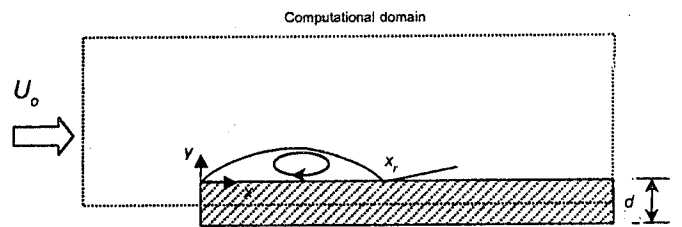


Figure 1: Computational domain and schematic of mean flow around a two-dimensional bluff plate.

## 3. The Unsteady Separated Flow around a Bluff Rectangular Plate

The prediction of turbulent flows with large regions of separation remains one of the most challenging problems in fluid dynamics. Such flows are encountered in a large variety of applications ranging from turbine blades, to buildings and heat exchangers. The unsteady flow over a bluff rectangular plate is a particularly attractive benchmark configuration that simplifies the study of separated and reattaching flows, particularly from a numerical

standpoint. This flow configuration, shown in Figure 1. For sufficiently large Reynolds numbers, the separating shear layer becomes unstable, and transition to turbulence occurs soon after separation. Further downstream, the free shear layer interacts with the surface of the plate and eventually reattaches. The separation process is often accompanied by what has been termed as "flapping" a low frequency motion with characteristic frequencies lower than those associated with the Kelvin-Helmholtz and the subsequent shear-layer roll-up. In the reattachment region, the flow is characterized by large scale unsteadiness, and pseudo-periodic bursting of the separation bubble and shedding of vorticity [9,10]. Further downstream, the reattached boundary layer does not recover to equilibrium conditions until allowed to redevelop over a long distance. These phenomena have a profound effect on the dynamics of the flow and on the transport of momentum, heat and other scalars, and are at the origin of many of the difficulties encountered by turbulence models.

In the present investigation, numerical results of the flow over a bluff rectangular plate were taken from previous studies. This includes 2-D unsteady and 3-D unsteady simulations with DNS and LES techniques in a wide range of Reynolds numbers [4].

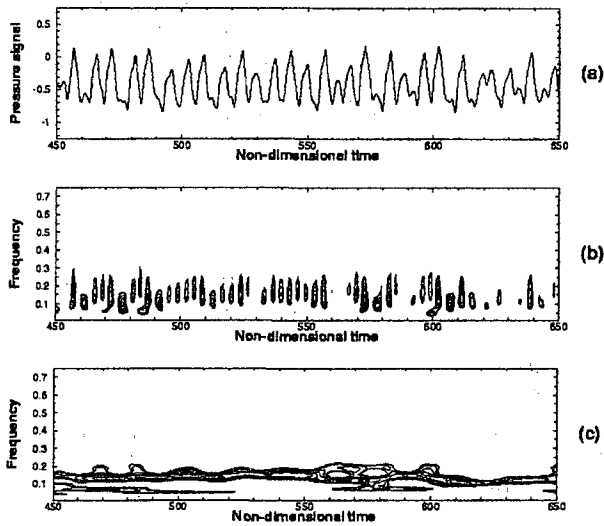


Figure 2: (a) Pressure signal at  $x/d = 2.0$ ,  $y/d = 0.5$ , (b) Mexican wavelet map, (c) Morlet wavelet map

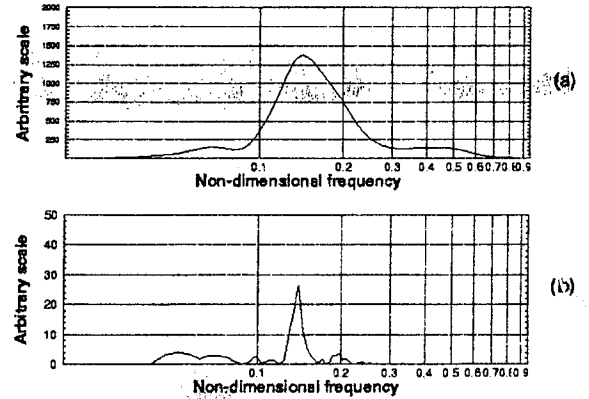


Figure 3: Mean power spectrum of pressure signal at  $x/d = 2.0$ ,  $y/d = 0.5$ ; (a) Wavelet transform, (b) Fourier transform

#### 4. Results and Discussions

##### 4.1 Two-dimensional simulations

In two-dimensional simulations at moderate Reynolds number,  $Re_d = U_0 d / \nu = 1,000$ , the Kelvin-Helmholtz instability of the separated shear layer leads to the formation, merging and shedding of vortices in a pseudo-periodic pattern. The details of the flow dynamics and statistics have been documented [3,11]. Typically, the vortex fields can be clearly detected from the pressure signals. The passage of a vortex at a given streamwise location can be identified by the suction peak of the pressure occurring at the same streamwise location. These pressure signals are used in the current investigation for the analysis of vortex dynamics. Figure 2(a) shows the selected pressure signal at location  $x/d = 2.0$ ,  $y/d = 0.5$ .

The energy distribution among the various frequencies can be visualized on the wavelet map in Figure 2(b) and 2(c). The contour lines on both figures represent the high value of the wavelet coefficients. The resolution of the scales/frequencies and of time localization vary depending on the basis or mother function used in the wavelet transform. Here the Mexican wavelet, which provides good time localization and the Morlet wavelet, which provides good spectral resolution are used. With the Mexican wavelet, the peak and the valley (the core of vortex) of the pressure signal are identified. The periodic pattern is clearly illustrated by a continuous contour line in Figure 2c. The concentration of energy is mainly around the non-dimensional frequency ( $fd/U_0$ ) of 0.08-0.25. This frequency range corresponds to the dominant frequency characterizing the large scale shedding from the reattachment region. This range of values is in agreement with those obtained from Tafti and Vanka's autocorrelation analysis [11]. The corresponding Fourier and wavelet transform spectra are compared in Figure 3. The frequency peak obtained from both transforms is identical and is centered around the non-dimensional frequency ( $fd/U_0$ ) of 0.15

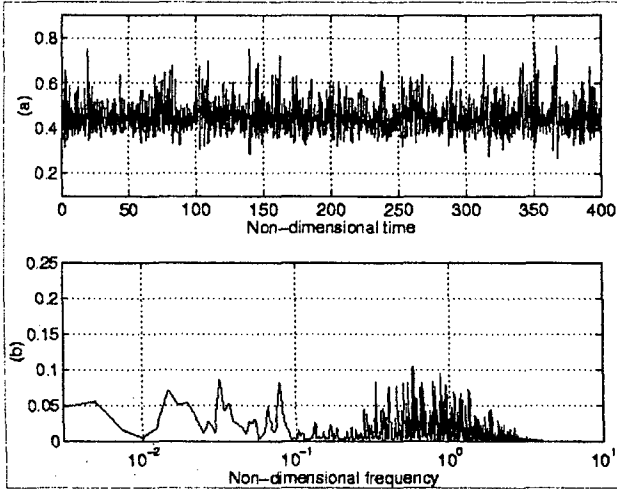


Figure 4: 3-D LES simulation (a) vertical velocity ( $v$ ) signal at  $x/d = 0.493$ ,  $y/d = 0.47$ , mid-span; (b) power spectrum density

#### 4.2 Three-dimensional simulations

In three-dimensional simulation performing with large eddy simulation (LES) at high Reynolds number,  $Re_d = 50,000$ , the trace of the instantaneous vertical velocity was recorded just downstream of separation within the shear layer and shown in Figure 4(a). The power density spectrum of this signal is shown in Figure 4(b). Consistent with experimental spectra [10], high frequency motion is dominant in the vicinity of separation, and the spectrum indicates small eddies with time scales of order of  $0.3 tU_o/d$ . In addition to the high frequency activity centered around  $fd/U_o = 0.8$ , the signal also exhibits peaks in the low frequency range ( $fd/U_o \approx 0.02-0.08$ ). From previous studied [9, 10], this low frequency motion is attributed with the flapping of the shear layer.

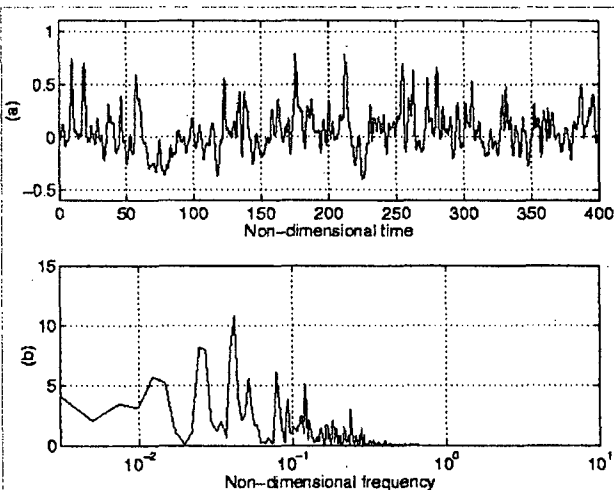


Figure 5: 3-D LES simulation (a) near-wall streamwise velocity ( $u$ ) signal at  $x/d = 4.51$ , mid-span; (b) power spectrum density

To provide further insight into the flow dynamics around the reattachment region, Figure 5(a) shows the streamwise velocity signal at a location close to the mean reattachment ( $\bar{x}_r$ ) and the corresponding power density spectrum. Compared to the signal sampled near separation in Figure 4, there is little energy in the high frequencies. Most of the energy is in the larger scales corresponding to non-dimensional frequencies ( $fd/U_o$ ) well below 0.2.

A time domain analysis using the wavelet transform of the near-wall streamwise velocity signal was conducted in this region. Figure 6 shows the wavelet map of this signal, in terms of the relief plot of the absolute value of the wavelet coefficient. The intermittent nature of the large scale unsteadiness is illustrated along the most distinct range of scales:  $tU_o/d \approx 20-50$ . This range corresponds to non-dimensional frequencies of 0.02-0.05 and is associated with the low frequency flapping of the shear layer. The intermittence of this phenomenon is clearly shown by the alternating peaks and troughs between 45 and 395 time units. The scales containing the most energy are in the range of  $5-15 tU_o/d$ , or non-dimensional frequencies of 0.066-0.2. This coincides with the range of frequencies reported experimentally for the pseudo-periodic vortex shedding around reattachment [10].

The time localization of these events shows activity of relatively short duration, followed by longer quiescent periods. Furthermore, the signal in Figure 6a shows positive fluctuations about the mean which are of a much higher amplitude than the negative fluctuations. This feature and the patterns shown in the wavelet map suggest that a typical cycle consists of two distinct phases: (i) gradual growth of large scale structures in the separated shear layer, accompanied by a progressive growth of the separation bubble; (ii) shedding of a large scale structure followed by a "collapse" of the bubble and abrupt shortening of the reattachment length.

For structure identification, the instantaneous vorticity field,  $|\omega|$  techniques, is plotted in Figure 7. In this figure, the structures close to separation are hardly discernible, however, three horseshoe vortices are visible in the reattachment region.

In order to identify the flow structures more clearly, the technique of Jeong and Hussain [8] was used. The contour plot of the second largest eigenvalue ( $\lambda_2$ ) is plotted in Figure 8 for the same instantaneous fields as Figure 7. In Figure 8, the structures are much more clearly exhibited than in Figure 7. In the first half of the mean separation bubble,  $x/d \leq 2$ , the strong background shear along the separated shear layer is eliminated and only vortex cores remain. These structures develop at the leading edge of the plate and are largely two-dimensional in nature. Further downstream, in the reattachment region, three-dimensionalization has occurred and the predominant structures are clearly identified as hairpin (horseshoe)

vortices. These structures are identical to the sketch suggested by Kiya and Sasaki [9] based on the interpretation of conditionally sampled data. The spanwise length scale of the horseshoe vortices in the reattachment region range from 1.5d to 2.75d which is in the range suggested in [9, 12].

### 5. Concluding Remarks

In two-dimensional simulations of the unsteady separated flow over a bluff rectangular plate at moderate Reynolds number of 1,000, the continuous wavelet transform offers an alternative approach to the problem of identifying and detecting the flow structures from the pressure fluctuations of the flow. This approach directly identifies the dominant time scales and the periodicity of the signal at any location (time) in the signals. In three-dimensional simulation at high Reynolds number, the intermittent nature of the flow can also be deduced from the wavelet analysis. The characteristic frequencies obtained from the simulations are in good agreement with spectral analysis of experimental signals.

In three-dimensional simulation at  $Re_d = 50,000$ , the flow structures break up and become turbulent right after the separation. The horseshoe vortices are identified in the reattachment region. This structure is more clearly identified with the  $\lambda_2$  technique than with the typical  $|\omega|$  technique, and identical to the sketch suggested by Kiya and Sasaki [9]. With Fourier and wavelet transforms analysis, the characteristic frequencies and intermittent nature of the pseudo-periodic vortex shedding from the separated shear layer and the reattachment region as well as the shear layer flapping were captured.

### 6. References

- [1] J.P. Bonnet, J. Lewalle and M.N. Glauser, "Coherent structure: past, present and future", *Advances in Turbulence IV*, Kluwer Academic Publishers, 1996, pp. 83-90.
- [2] G.L. Brown and A. Roshko, "On density effects and large structure in turbulent mixing layer", *Journal of Fluid Mechanics*, Vol. 63, 1974, pp. 775-816.
- [3] J. Jeong and F. Hussain, "On the identification of vortex", *Journal of Fluid Mechanics*, Vol. 285, 1995, pp. 69-94.
- [4] A. Suksangpanomrung, "Investigation of unsteady separated flow and heat transfer using large eddy simulation", Ph. D. dissertation, University of Victoria, Canada, 2000.
- [5] M. Farge, "Wavelet transform and their application to turbulence", *Annu. Rev. Fluid Mech.*, Vol. 24, 1992, pp. 395-457.
- [6] H. Higuchi, J. Lewalle and P. Crane, "On the structure of a two-dimensional wake behind a pair of flat plates turbulent flow around a bluff rectangular plate", *Physic of Fluids*, Vol. 6(1), 1994, pp. 297-305.
- [7] T. Dallard and F. K. Browand, 1993, "The growth of large scales at defect sites in the plane mixing layer", *Journal of Fluid Mechanics*, 1993, Vol. 247, pp. 339-368.
- [8] J. Jeong, F. Hussain, W. Schoppa and J. Kim, "Coherent structure near the wall in a turbulent channel flow", *Journal of Fluid Mechanics*, Vol. 332, 1997, pp. 185-214.
- [9] M. Kiya and K. Sasaki K., "Structure of large-scale vortices and unsteady reverse flow in the reattaching zone of a turbulent separation bubble", *Journal of Fluid Mechanics*, 1985, Vol. 154, pp. 463-491.
- [10] N. Djilali and I.S. Gartshore, 1991, "Turbulent flow around a bluff rectangular plate. Part I: Experimental investigation", *Journal of Fluids Engineering*, 1991, Vol. 113, pp. 51-59.
- [11] D.K. Tafti and S.P. Vanka, "A numerical study of flow separation and reattachment on a blunt plate", *Physic of Fluids*, Vol. A3(7), 1991, pp. 1749-1759.
- [12] P.J. Saathoof and W.H. Melbourne, "Effect of free stream turbulence on surface pressure fluctuations in a separation bubble", *Journal of Fluid Mechanics*, 1997, Vol.337, pp. 1-24.